Article

A Ratiometric Electrochemiluminescent/Electrochemical Strategy for Sensitive Detection of MicroRNA Based on Duplex-Specific Nuclease and Multilayer Circuit of Catalytic Hairpin Assembly

Liping Zhu, Mengqian Zhang, Jing Ye, Mengxia Yan, Qiuju Zhu, Jianshe Huang, and Xiurong Yang

Anal. Chem., **Just Accepted Manuscript** • DOI: 10.1021/acs.analchem.0c01949 • Publication Date (Web): 26 May 2020

A Ratiometric Electrochemiluminescent/Electrochemical Strategy for Sensitive Detection of MicroRNA Based on Duplex-Specific Nuclease and Multilayer Circuit of Catalytic Hairpin Assembly

Liping Zhu, [†] *Mengqian Zhang,* [†] *Jing Ye,* [†] *Mengxia Yan,* [†,‡] *Qiuju Zhu,* [†] *Jianshe Huang,* [*,‡] *and Xiurong Yang* [*,†,‡]

[†]Department of Chemistry, University of Science and Technology of China, Hefei, Anhui 230026, P. R. China

[‡]State Key Laboratory of Electroanalytical Chemistry, Changchun Institute of Applied Chemistry, Chinese Academy of Sciences, Changchun, Jilin 130022, P. R. China

KEYWORDS: Ratiometric biosensor, Electrochemiluminescence, Duplex-specific nuclease, Catalytic hairpin assembly, Cascade amplification, MicroRNA-499

ABSTRACT: In this study, we proposed a ratiometric electrochemiluminescent (ECL) /electrochemical (EC) biosensor based on duplex-specific nuclease (DSN)-assisted target recycling and multilayer catalytic hairpin assembly (CHA) amplification cascades for the detection of microRNA (miRNA). The DSN-assisted target recycling transformed miRNAs into a large number of ssDNA, which then catalyzed multilayer CHA amplification cascade to produce numerous long dsDNA duplexes H_n/H_{n+1} (n=2, 4, 6…). Then the H_n/H_{n+1} displaced the ferrocene (Fc)-labeled ssDNA (S_{x+1}, x=1, 3, 5…) to hybridize with the S_x sequence on the gold electrode surface. Consequently, a

great number of long $S_x/H_n/H_{n+1}$ duplexes were immobilized for binding $Ru(phen)_3^{2+}$ to obtain an amplified ECL signal. Meanwhile, the EC signal of Fc reduced, and the quenching effect of Fc to ECL signal also decreased. By measuring the ratio of ECL signal of $Ru(phen)_3^{2+}$ to EC signal of Fc, quantitative analysis of miRNA-499 with high accuracy and reproducibility was obtained. The ratiometric biosensor shows high sensitivity and a wide linear range of six orders of magnitude. With the help of DSN-assisted target recycling, this strategy can be easily extended to detect other miRNAs without redesigning the CHA cascade system. The proposed "hybrid" ratiometric ECL/EC strategy enriches the ratiometric sensors, and can find extensive applications in bioanalysis, especially for multiplex detection.

INTRODUCTION

Ratiometric electrochemiluminescence (ECL) assays with dual-signal outputs can effectively overcome the potential interference from the complex environment and improve the accuracy of detection.[1-3] Typical ECL ratiometry is based on the ratio of two luminescence signals for quantitative analysis. For example, based on the luminescence signal pairs at different wavelengths or different potentials, the corresponding wavelength-resolved[4-7] or potential-resolved[8-13] ratiometric ECL biosensors were constructed to quantify protein, ion, DNA, microRNA and cell. Meaningfully, a novel ratiometric strategy based on the ratio of ECL to electrochemical (EC) signal was recently developed.[14] In the ratiometric ECL/EC system, ECL signal is usually used as a working signal that changes with the concentration of the target,

while the electrochemical signal can be either a reference signal[15-17] independent of the analyte or a working signal[14] dependent on the analyte. Compared with the wavelength-resolved and potential-resolved ratiometric ECL biosensors, the ECL/EC ratiometric method not only has the typical advantages of low background and high accuracy of the ECL ratiometric biosensor, but also has the characteristic of simple operation and wide applicability. For instance, in wavelength-resolved ECL ratiometry, the ECL spectra of luminophores are usually gained through a series of optical filters[4] or an additional coupled spectrophotometer,[18] which is tedious and time consuming. While potential-resolved ECL ratiometry[8,10] usually needs a wide scanning potential, and it is difficult to select a shareable coreactant for the pair of anodic/cathodic emitters. Although ratiometric ECL/EC strategy has more advantages than the ratiometric biosensors with dual-luminescence signal outputs, its development is still in infancy, and there are only a few reports on ECL/EC biosensors.[14-17] Therefore, it is of great significance to develop ratiometric ECL/EC biosensors with excellent performance for biological analysis.

Catalytic hairpin assembly (CHA), an efficient isothermal enzyme-free amplification method, was first proposed in 2008,[19] and has been extensively studied for sensitive biological analysis.[20,21] In a typical CHA reaction, two complementary strands of DNA are designed into hairpin structures and the complementary domains are locked in the hairpin stems. When a single-strand nucleic acid (the initiating strand) appears, toehold-mediated strand displacement (TMSD) is triggered, and the two

hairpins are successively opened and rapidly form the thermodynamically optimal DNA duplex. Furthermore, through reasonable sequence design, the DNA duplex of the first CHA reaction can trigger another pair of DNA hairpins to form a new DNA duplex, realizing the cascading of the CHA reaction.[22] MicroRNAs (miRNAs) are a kind of endogenous, non-coding, single-stranded RNAs with approximately 19-23 nucleotides,[23,24] which are suitable for directly triggering CHA reactions to realize their sensitive detection. However, in order to obtain high detection sensitivity and to overcome the limitation of miRNAs degradation, miRNAs are often converted into DNA strands that acted as trigger strands.[21] An efficient and simple method to do this is to use duplex-specific nuclease (DSN), which can hydrolyze double-stranded DNA with more than 10 bp or DNA in DNA/RNA hybridization chains.[25,26] Combining DSN amplification with CHA circuits can not only sensitively detect low abundance miRNAs in biological samples, but can also be conveniently extended to the detection of other miRNAs without redesigning the strands used in CHA reactions.[27-29]

Although CHA circuits have been widely adopted for constructing various types of biosensors, including fluorescent,[30-33] electrochemical,[34] chemiluminescent[35] and colorimetric biosensors,[36] the application of this method to improve the detection performance of ECL biosensors remains largely unexplored. Hence, we used miRNA-499, a potential biomarker of acute myocardial infarction (AMI),[37-39] as the model target to construct a ratiometric ECL/EC biosensor based on DSN-assisted target recycling and multilayer CHA amplification cascade. As shown in Scheme 1, the

S_x/S_{x+1}(x=1, 3, 5…) hybrids were first anchored on the surface of the gold electrode (GE) via Au-S bond. Ferrocene (Fc) was labeled on S_{x+1} as the EC probe, and also acted as a quenching agent for ECL signal of $Ru(phen)_3^{2+}$ through the electron transfer between excited-state $Ru(phen)_3^{2+*}$ and Fc^+.[40,41] In the absence of target, a small amount of $Ru(phen)_3^{2+}$ can be embedded in the S_x/S_{x+1} hybrids, and Fc^+ will efficiently quench the ECL signal, thus reduce the background interference. After DSN-assisted target recycling amplification, the target miRNA was converted into a large number of ssDNA for triggering multilayer CHA amplification cascade to produce a series of long H_n/H_{n+1}(n=2, 4, 6…) dsDNA duplexes. Then H_n/H_{n+1} displaced S_{x+1} by strand displacement reaction to form $S_x/H_n/H_{n+1}$ hybrids for intercalating $Ru(phen)_3^{2+}$ molecules. Thus, a strong ECL signal and a reduced EC signal were obtained and a ratiometric RNA biosensor based on the ECL/EC was developed. The proposed ratiometric biosensor shows excellent analytical performance and can be successfully used for miRNA-499 detection in human serum samples, demonstrating its great promising perspective in bioanalysis.

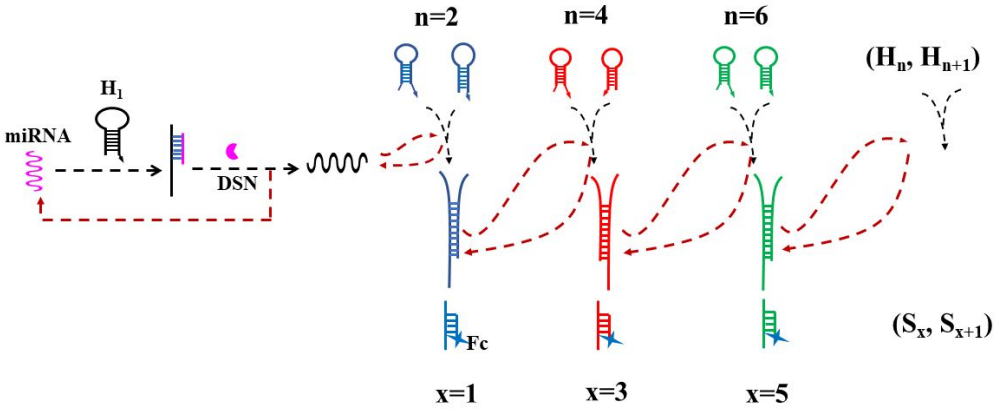

Scheme 1. Schematic illustration of DSN-assisted target recycling and multilayer CHA amplification cascade.

EXPERIMENTAL SECTION

DSN-Assisted Target Recycling Amplification and Multilayer CHA Amplification Cascade. Prior to commencing the series of reaction, all the hairpin DNAs were heated to 95 °C for 2 min, and then cooled to room temperature at a cooling rate of 6 ℃/min. 3 μL of H_1 solution (10 μM) was incubated with 3 μL of DSN (0.1 U/μL) and 6 μL different concentrations miRNA-499 at 50 °C for 70 min. Subsequently, 15 μL of 2×DSN stop solution (10 mM EDTA) was injected into above solution and reacted at 50 °C for 30 min, then rapidly heated the solution to 90 °C for 10 minutes to completely inactivate the DSN. The final solution was cooled down to 4 °C slowly. Next, 3 μL of hairpin DNA mixture of H_n and H_{n+1} (n=2, 4, 6…) (the concentration of each hairpin probe was 10 μM) was added and further reacted for 15 h at 4 °C to produce H_n/H_{n+1} hybrids. The resulting mixture was stored at 4 °C for further use.

Fabrication of the Ratiometric ECL/EC Biosensor. Briefly, the gold electrode (GE) (Φ = 3 mm) was pretreated with a piranha solution (98%H_2SO_4:30% H_2O_2 = 3:1) and polished sequentially with alumina powder (0.3 and 0.05 μm), and then ultrasonically cleaned with ethanol and ultrapure water. Then the GE was electrochemically scanned in 0.5 M H_2SO_4 solution to obtain the stable characteristic peaks and dried with N_2. Thiolated DNA strands S_x (2 μM) (x=1, 3, 5……) were incubated with TCEP (10 mM) in Tris-HCl buffer (pH 8.0) for 30 min at 37 °C, respectively. Afterwards, equal volume

of the S_x (2 μM) and Fc-labeled S_{x+1} (2.25 μM) were mixed together and incubated at 4 °C for 2 h to obtain S_x/S_{x+1} duplex. Next, 10 μL of the mixture of S_x/S_{x+1} (1 μM) was dropped on the surface of the cleaned GE and incubated at 4 °C for 8 h. The (S_x/S_{x+1})/GE was further incubated with 4 μL of MCH solution (1 mM) at 4 °C for 1 h to block the unspecific sites. Subsequently, 10 μL of resulting mixture of DSN-assisted target recycling and multilayer CHA amplification cascades was casted on the surface of the modified electrode to react at 37 °C for 2 h. Finally, 10 μL of $Ru(phen)_3^{2+}$ (1 mg/mL, dissolved in 0.1 M PBS solution) was spread on electrode surface to react at 37 °C for 2 h. It should be noted that the electrode needed to be rinsed with PBS buffer 5 times after each modification step.

Measurement of ECL and EC Signals. The ECL and square wave voltammetry (SWV) signals were measured in PBS solution (0.1 M, pH = 7.4) containing 20 mM 2-(dibutylamino)ethanol (DBAE) and 0.1 M KCl at room temperature. Gold electrode was used as working electrode, a saturated calomel electrode acted as reference electrode and a platinum wire was the auxiliary electrode. The scanning potential for ECL was in the range of 0 to 1.4 V with a scan rate of 100 mV/s, and the voltage of photomultiplier tube (PMT) was set at 900 V unless otherwise stated. SWV measurements were performed from 0.5 to -0.15 V, the modulation amplitude was 25 mV and the step potential was 4 mV. We firstly measured the ECL signal and then immediately performed negative potential scanning to obtain SWV signal. Unless

otherwise stated, the error bars in this paper represented the standard deviation (SD) for three parallel measurements.

RESULTS AND DISCUSSION

Principle of the Proposed ECL/EC Ratiometric Biosensor. As shown in Scheme 2, the principle of the proposed ECL/EC ratiometry with two-layer CHA circuits as an example was illustrated. Mercapto-labeled S_1 and S_3 (Table S1) combined with Fc-labeled S_2 and S_4 to form the S_1/S_2 and S_3/S_4 hybrids, which were self-assembled on the surface of the GE. miRNA-499 was completely complementary to the loop of H_1 (a hairpin DNA with 7 base pairs in the stem) to form RNA/DNA hybrid. After adding DSN, the complementary DNA sequence to miRNA-499 in RNA/DNA hybrid was hydrolyzed into pieces, and the remaining sequence containing 27 bases was released as a trigger chain (T), target miRNA-499 was also released for a new cycle of DSN cleavage reaction. Thus, through the DSN digestion circuit, a small amount of miRNA-499 can produce a large number of trigger chains. T first combined with the overhang of hairpin H_2, and opened the hairpin structure to expose a toehold which can hybridize with the sticky end of hairpin H_3. Finally, H_2/H_3 hybrids were formed and trigger chains were recycled. Next, the overhang domain of H_2 in H_2/H_3 hybrid can act as the catalytic chain to bind with the toehold of H_4 to form $H_2/H_3/H_4$, and then the newly exposed overhang of H_4 hybridized with the sticky end of H_5 to release H_2/H_3 hybrid and form H_4/H_5 duplex, thus completing the two-layer CHA cascade amplification. The above series of reactions were performed in the centrifuge tube, the final reaction products

H_2/H_3 and H_4/H_5 hybrids were dropped on the surface of the S_1/S_2 and S_3/S_4 modified GE. The overhang part of H_2 and H_4 first hybridized with the exposed domain of S_1 and S_3, respectively, and then replaced Fc-labeled S_2 and S_4 through branch migration[42] to form $S_1/H_2/H_3$ and $S_3/H_4/H_5$. These large numbers of long dsDNAs ($S_1/H_2/H_3$ and $S_3/H_4/H_5$) can be used as carriers for embedding $Ru(phen)_3^{2+}$ to obtain a strong ECL signal. At the same time, with the displacement of S_2 and S_4 on the electrode surface, the EC signal of Fc and the quenching effect on ECL signal also decreased. Consequently, by measuring the ratio of the ECL signal of $Ru(phen)_3^{2+}$ to the EC signal of Fc, a sensitive and accurate ratiometric ECL/EC biosensor for detecting miRNA-499 was established.

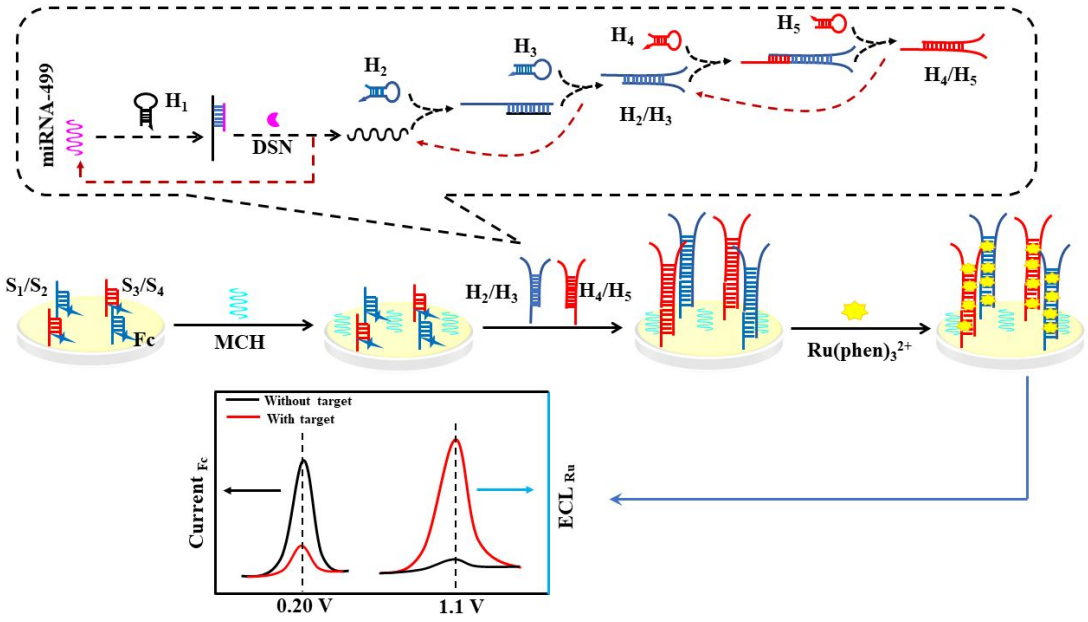

Scheme 2. Schematic illustration of ECL/EC ratiometric biosensor.

Optimization the Number of Layers of CHA Amplification Cascade. Circuit leakage caused by initiator-independent reactions will produce certain background signals, while linear multi-layer amplification cascades will make the background

signals be amplified layer by layer, resulting in a severe decrease in sensitivity.[22,43] Signal to noise ratio (S/N) represents the sensitivity of the sensors and determines the detection limit. However, there are many factors that influence the S/N of the system, such as the characteristics of the used instruments, the diversity of experimental operations and the performance of the system's detection strategy. Signal-to-background ratio (S/B) can well reflect the performance of the detection strategy used in sensor, especially in molecular signal amplification technology.[22] Therefore, in order to obtain better sensitivity of the biosensor, we studied the S/B of different layer CHA circuits and selected the optimal high-quality DNA circuit. As shown in Figure 1A, from one-layer CHA circuit to four-layer CHA circuit, the time required to complete the reaction increased significantly. When the reaction time of these CHA circuits was 3 h, 5 h, 9 h and 14 h, respectively, the ECL signal tended to level-off. Therefore, we chose 3 h, 5 h, 9 h and 14 h as the optimal reaction times for one-layer to four-layer CHA circuit, respectively. The ECL signal for different layer CHA circuits at the optimal reaction time was 1094, 4164, 7367 and 10121 a.u., respectively. Meanwhile, their corresponding background signal was 128, 197, 907 and 2008 a.u. (Figure 1B), respectively. In addition, when target miRNA hybridized with H_1 and then directly reacted with the S_c/S_{c1} (the sequences of S_c and S_{c1} was shown in Table S1) without DSN-assisted target recycling amplification and multilayer CHA amplification cascade, the background signal and the ECL signal was 55 and 71 a.u., respectively. The calculated S/B of different layer circuits is shown in Figure 1C. Obviously, the two-

layer CHA circuit had the highest S/B. Furthermore, according to these experimental results, we can also obtain the signal amplification factor (AF, the ratio of ECL signal with and without CHA circuit) of different layer CHA circuits. The AFs from one-layer to four-layer CHA circuits were calculated to be about 60, 250, 400 and 510, respectively, showing that the amplification factor increased slowly in the higher layer than the two-layer CHA circuit. According to the above results, it can be seen that two-layer CHA circuit shows a good signal amplification efficiency and an excellent S/B ratio, which ensured the sensitivity of the system and moderate reaction time. Consequently, two-layer CHA circuit was selected as the optimal cascade architecture for amplifying signal.

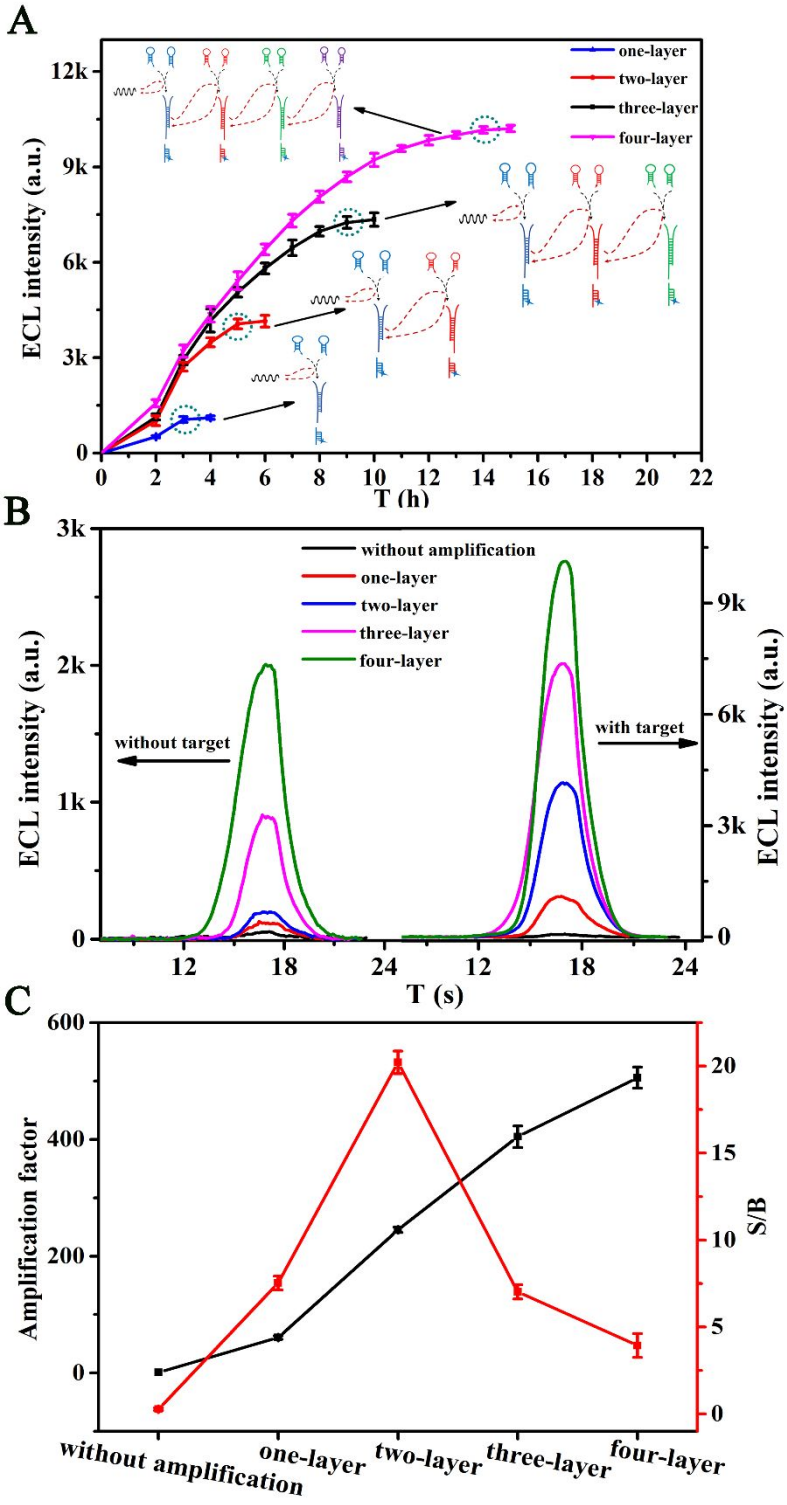

Figure 1. Optimization the number of layers of CHA amplification cascade. (A) ECL intensity-time curves for different layer CHA reactions. (B) ECL responses of different amplification systems in the presence or absence of target miRNA. (C) Amplification

factors and S/B ratios of different amplification systems. The concentration of miRNA-499 was 100 pM, and PMT was set at 700 V.

Native polyacrylamide gel electrophoresis (PAGE) was used to evaluate the cascade amplification system. As shown in Figure S1, when the target miRNA hybridized with H_1 to form miRNA/H_1 hybrid (lane 2), the migration rate decreased. However, after the DSN-assisted target recycling (lane 4), almost all the miRNA/H_1 were effectively cleaved. The target miRNA and trigger chain (T) containing 27 bases were released (because of their relatively small molecular weight, they had run out of the lane). After the resulting mixture of DSN-assisted target recycling reacted with H_2, a higher stripe appeared in lane 6, indicating that the T/H_2 was formed. T/H_2 then reacted with H_3, (H_3+H_4) and (H_3+H_4+H_5) and formed H_2/H_3 (lane 8), H_2/H_3/H_4 (lane 10) and mixture of H_2/H_3 and H_4/H_5 (lane 12). The location of stripes was consistent with our expectation, confirming the rationality of our cascade architecture.

Characterization of the Ratiometric ECL/EC Biosensor. To successfully construct a ratiometric ECL/EC biosensor, the desired EC signal should have good potential resolution with the signals of other electrochemical active substances in the system. As shown in Figure 2A, the SWV peak of Fc was located at about 0.20 V, which was dramatically different from the initial potential and peak potential of $Ru(phen)_3^{2+}$ and the coreactant DBAE, indicating that it was feasible to use Fc and $Ru(phen)_3^{2+}$ as EC and ECL tags to develop ratiometric ECL/EC biosensor. Figure 2B shows the typical EC and ECL responses of the developed biosensor before and after the addition of target

miRNA. In the absence of target, the biosensor shows strong EC signal at 0.2 V and very weak ECL signal at 1.1 V. With the addition of the target and the increase of concentration, the EC signal gradually decreased, while the ECL signal significantly increased, indicating that in this system, both the EC signal and the ECL signal were target-dependent and consistent with our design. The remarkable increase in ECL intensity was attributed to the generation of a large number of long dsDNA ($S_1/H_2/H_3$ and $S_3/H_4/H_5$) for the intercalation of $Ru(phen)_3^{2+}$ on the one hand, and on the other hand, the decrease of S_2 and S_4 on the electrode surface weakened the quenching effect of Fc on ECL signal of $Ru(phen)_3^{2+}$.

As shown in Figure 2C and 2D, CV and EIS experiments were performed to characterize the assembly process of the ratiometric biosensor. The bare GE showed a symmetrical redox peak with a high peak current (Figure 2C, curve a) and a small impedance of about 100 Ω (Figure 2D, curve a). When S_1/S_2 and S_3/S_4 duplexes anchored on the GE surface, the peak current (Figure 2C, curve b) decreased and the impedance (Figure 2D, curve b) increased due to the repulsive interaction between the negatively charged DNA molecules and the $[Fe(CN)_6]^{3-/4-}$ pair. The modification of MCH on the electrode, further caused the reduced peak current and the increased resistance because the compact self-assembly layer impeded the electrochemical probes to approach the electrode surface (curve c in Figure 2C and 2D). After the products of DSN-assisted target recycling and two-layer CHA amplification cascade were modified on the electrode surface, the peak current decreased significantly with a large separation

of redox peaks (Figure 2C, curve d), and the impedance increased dramatically (Figure 2D, curve d). The result was ascribed to the fact that a large number of long dsDNA ($S_1/H_2/H_3$ and $S_3/H_4/H_5$) was formed on the electrode surface, proving that the biosensor was successfully fabricated.

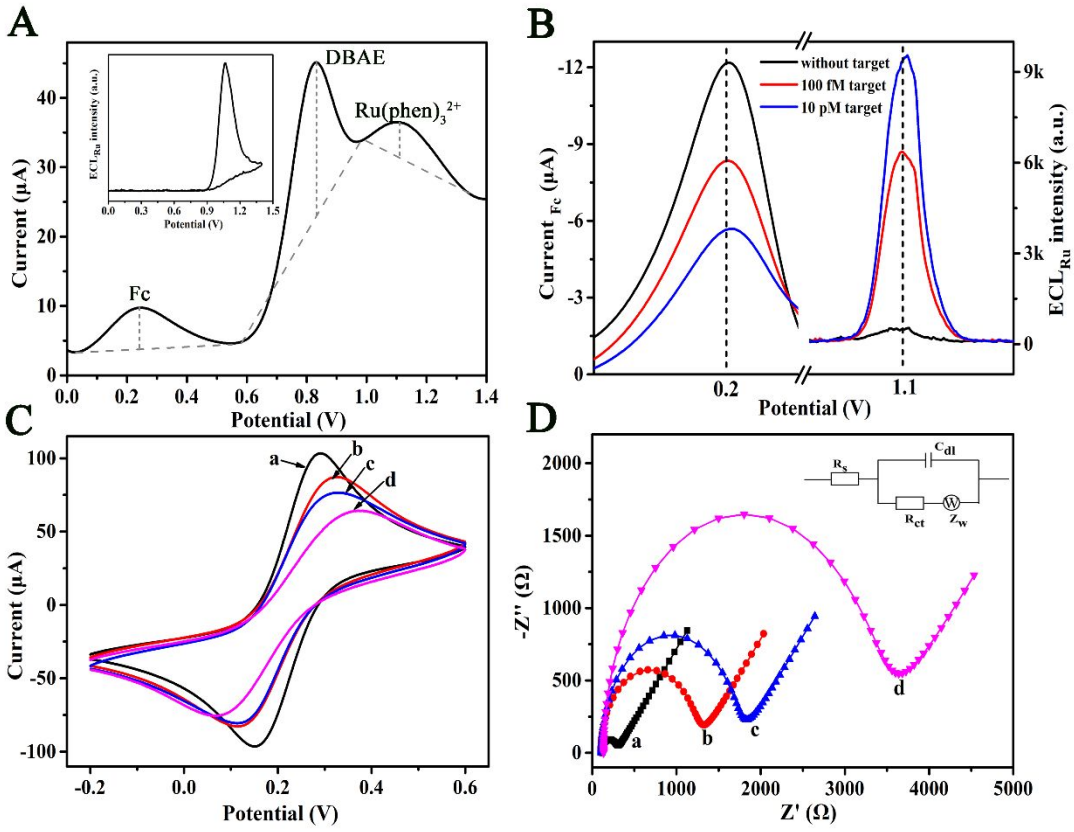

Figure 2. (A) SWV response of the ratiometric biosensor, the concentration of miRNA-499 was 100 fM. Inset shows the ECL-potential curve of the biosensor. (B) The ECL and SWV responses before and after the addition of the target. (C) CV and (D) EIS curves of the biosensor assembly process: (a) GE, (b) (S_1/S_2 and S_3/S_4)/GE, (c) MCH/(S_1/S_2 and S_3/S_4)/GE and (d) (H_2/H_3 and H_4/H_5)/MCH/(S_1/S_2 and S_3/S_4)/GE in 5 mM $[Fe(CN)_6]^{3-/4-}$ solution containing 0.1 M KCl. The scan rate for CV was 100 mV/s,

the concentration of miRNA-499 was 100 pM. Inset is equivalent circuit of the biosensor.

Optimization of Experimental Conditions. For excellent detection performance of the biosensor, the time for DSN cleavage reaction, the incubation time for mixture solution of H_2/H_3 and H_4/H_5 with S_1/S_2 and S_3/S_4 modified electrode, as well as the time for binding of $Ru(phen)_3^{2+}$ were optimized. As shown in Figure S2A, with the increase of reaction time for DSN-assisted target recycling, the ECL signal increased rapidly, accompanied by the decline of EC signal. After 70 min reaction, both EC and ECL signal leveled off. Therefore, 70 min was selected as the optimal reaction time for DSN cleavage reaction. The effect of incubation time between H_2/H_3, H_4/H_5 hybrids and S_1/S_2, S_3/S_4 modified electrode was also investigated (Figure S2B). The ECL signal raised while the EC signal decreased rapidly with the increase of incubation time, and both of them reached a plateau at 120 min, indicating the appropriate incubation time was 120 min. In addition, the ECL intensity enhanced with the increase of time for intercalation of $Ru(phen)_3^{2+}$ and reached a maximum value at 120 min (Figure S2C), showing that the intercalation for $Ru(phen)_3^{2+}$ has reached an equilibrium. Accordingly, 120 min was selected as the optimal intercalation time.

Analytical Performance of the ECL/EC Ratiometric Biosensor. Under the optimized reaction conditions, we investigated the analytical performance of the constructed ECL/EC ratiometric biosensor for miRNA-499. As shown in Figure 3A, as the concentration of miRNA-499 increased from 0 aM to 100 pM, the ECL intensity

gradually enhanced and linearly correlated to miRNA-499 concentration from 10 aM to 100 pM, and the corresponding correlation coefficient (R^2) was 0.9973 (Figure 3B, black curve). While the EC signal of Fc gradually decreased (Figure 3A), and a linear range from 100 aM to 100 pM was obtained, the R^2 was 0.9912 (Figure 3B, blue curve). This result shows that ECL method is superior to EC method, exhibiting a wider linear range in this system. By using the ratio of ECL intensity to electrochemical current (I_{ECL}/I_{EC}) as the output signal (Figure 3C), the ratiometric biosensor exhibited an excellent linear relationship between the logarithm of I_{ECL}/I_{EC} and logarithm of miRNA-499 concentration in the range of 100 aM to 100 pM (R^2=0.9993). The limit of detection (LOD) of the proposed ECL/EC ratiometric biosensor for miRNA-499 was calculated to be 28.75 aM (S/N=3). Compared with other reported ECL or electrochemical miRNA biosensors, the ratiometric ECL/EC biosensor shows superior or comparable performance in terms of the detection limit and linear response range (Table S2), showing that the developed ratiometic biosensor had a great application prospect for miRNA-499 detection. More importantly, by simply replacing the complementary sequence of miRNA-499 in H_1 with that of other miRNA, the ratiometic biosensor can be immediately used for detecting the new target, demonstrating the universality of the developed method.

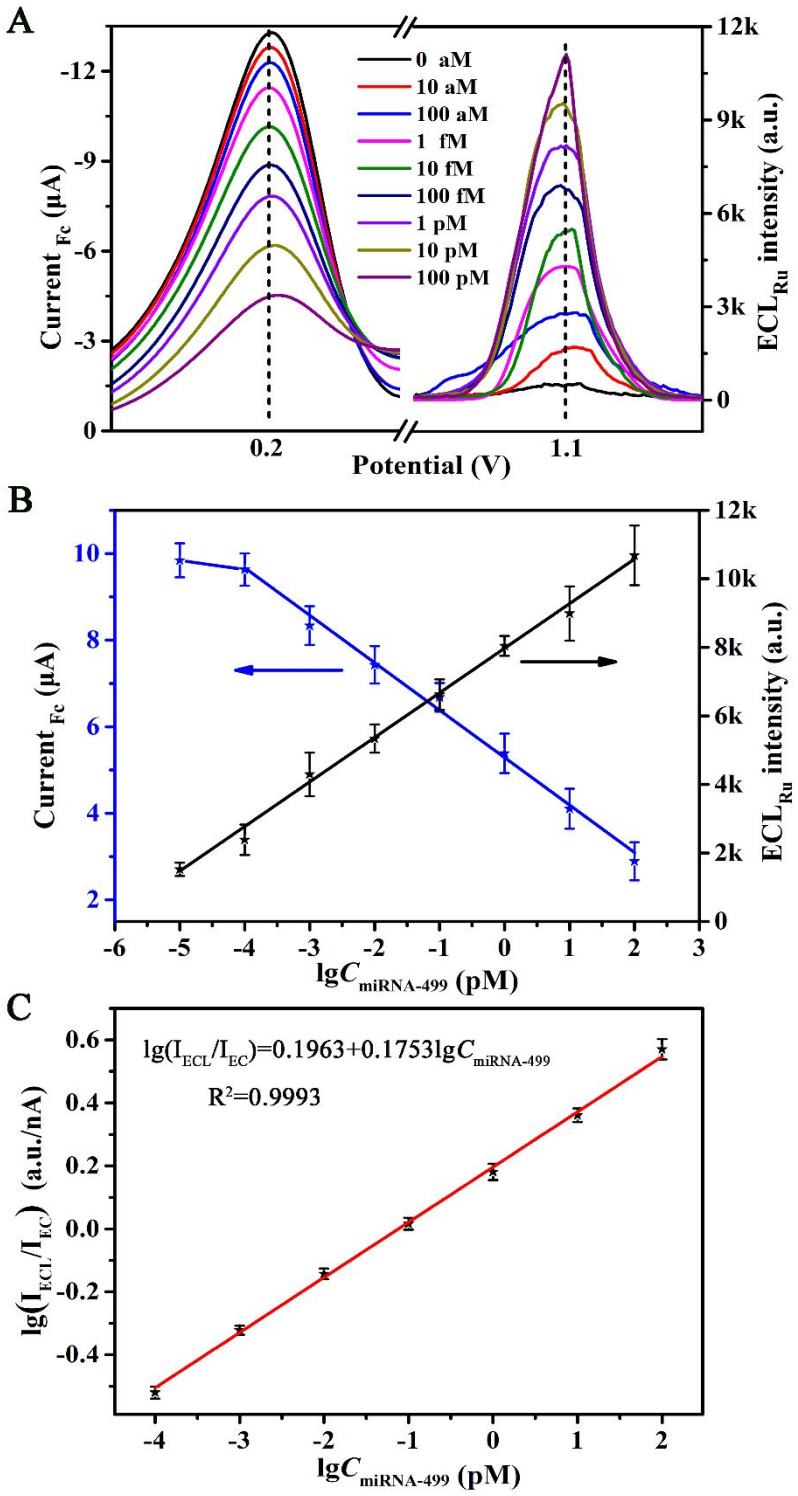

Figure 3. (A) ECL and SWV curves at different concentrations of miRNA-499. (B) Plots of ECL and EC signals versus lg$C_{miRNA-499}$ in the range of 10 aM-100 pM. (C) The calibration curve of lg(I_{ECL}/I_{EC}) vs. lg$C_{miRNA-499}$ at concentrations of 100 aM-100 pM.

Selectivity, Stability, Reproducibility of the Ratiometric Biosensor and Its Application in Real Sample Analysis. The selectivity of the ECL/EC ratiometric biosensor was evaluated by detecting miRNA-499 and other three kinds of miRNAs associated with acute myocardial infarction (miRNA-133a, miRNA-208b and miRNA-328) at the concentration of 10 times that of miRNA-499. As shown in Figure 4A, the I_{ECL}/I_{EC} ratios for the three interferences are similar to that of the blank, which are much smaller than that of the miRNA-499, indicating that the biosensor had good selectivity to the target. The stability was investigated by measuring the I_{ECL}/I_{EC} ratios of the ECL/EC ratiometric biosensor stored at 4 ℃ from 1 to 8 days. The I_{ECL}/I_{EC} ratio decreased merely by 5.72% from the first day to the fifth day (Figure 4B). It had 14.43% decline after 8 days storage. Furthermore, when the biosensor was continuously scanned for 33 cycles (Figure 4C), the ECL signal tended to be stable from the 6th cycle, and the relative standard deviation (RSD) of ECL signals for the remaining 28 cycles was 2.24%. All these results indicated that the ECL/EC ratiometric biosensor had a satisfactory stability.

To investigate the repeatability of the ECL/EC ratiometric biosensor, eight individual measurements for 100 fM target were conducted and the RSDs of the response values in the single-signal mode (ECL and EC) and ratiometric mode were analyzed (Figure 5A and 5B). The response signals of the ECL and EC showed large RSD of 10.01% and 8.94%, respectively. While the RSD of the ECL/EC ratios

markedly reduced to 2.27%, indicating that the ratiometric approach had much better reliability and repeatability than single-signal output approach.

In order to study the practicability of the ratiometric biosensor, we carried out the standard addition experiments by adding different concentrations of the miRNA-499 to 5% and 10% blank serum samples. As shown in Table 1, the recoveries ranged from 99.55% to 103.12% with the RSD of 1.58%-3.33%. These results clearly demonstrated that the constructed ratiometric biosensor had good accuracy for detecting miRNA-499 in real serum samples.

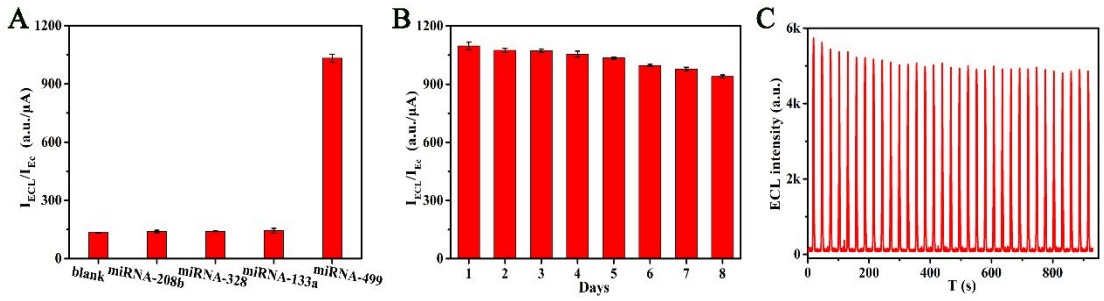

Figure 4. (A) The I_{ECL}/I_{EC} ratios of the blank, three interferences with a concentration of 1 pM and the target with a concentration of 100 fM. (B) The I_{ECL}/I_{EC} ratios of the biosensor at 1st day to 8th day, the concentration of miRNA-499 was 100 fM. (C) The ECL curves of the proposed biosensor under 33 successive cycles, the concentration of miRNA-499 was 5 fM.

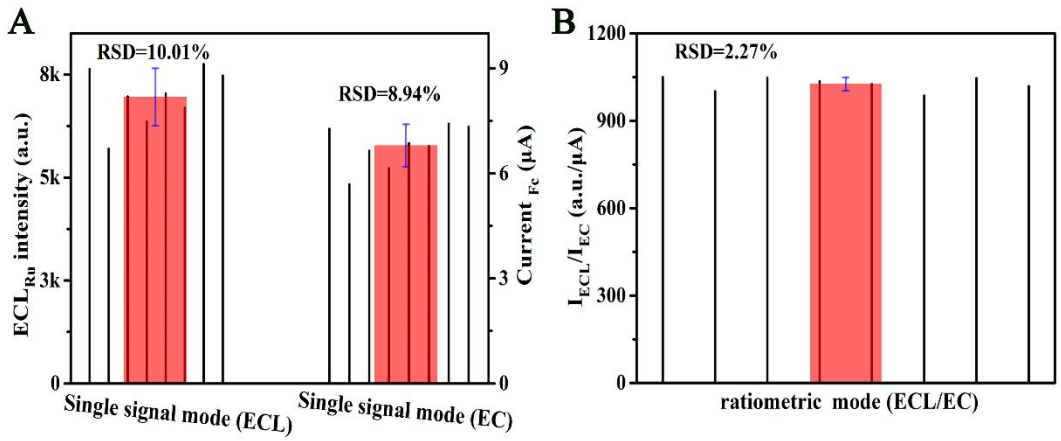

Figure 5. Repeatability analysis of (A) single-signal mode and (B) ratiometric mode.

Table 1. Recovery experiments for miRNA-499 detection in real human serum.

samples	spiked	found	RSD (%, n=3)	recovery (%)
Human serum (10%)	25 fM	25.78 fM	3.33	103.12
	250 fM	253.63 fM	2.98	101.45
	2.50 pM	2.49 pM	1.90	99.60
Human serum (5%)	25 fM	25.31 fM	2.11	101.24
	250 fM	248.87 fM	1.58	99.55
	2.50 pM	2.56 pM	1.91	102.40

CONCLUSIONS

In summary, a signal "hybrid" ratiometric biosensor was successfully developed for miRNA-499 detection by using the ECL signal of $Ru(phen)_3^{2+}$ and the EC signal of Fc. The large discrepancy between the oxidation potential of $Ru(phen)_3^{2+}$ and Fc could

avoid latent cross-interference. Benefiting from the DSN-assisted target recycling and the two-layer CHA amplification cascade, the constructed ECL/EC ratiometric biosensor showed high sensitivity for detection of miRNA-499 with the detection limit of 28.75 aM (S/N=3). The excellent accuracy, selectivity, reproducibility and stability of the ratiometric biosensor demonstrated its great potential for bioanalysis. Furthermore, DSN-assisted target recycling for converting miRNAs to DNAs allows the proposed biosensor to be immediately extended for analyzing various miRNAs by merely substituting for one DNA sequence (H_1). This feature makes the developed method a great application prospect in biosensing array for multiplex detection.

ASSOCIATED CONTENT

The Supplementary Materials is available free of charge on the ACS Publications website.

Reagents, apparatus, sequences of DNAs and RNAs used in this study, PAGE image of cascade amplification system used for constructing the ratiometric ECL/EC biosensor, figure of optimization of experimental conditions and comparison of different biosensors for miRNAs detection.

AUTHOR INFORMATION

Corresponding Author

* E-mail: xryang@ciac.ac.cn Tel.: +86 431 85262056; Fax: +86 431 85689278.

* E-mail: huangjs@ciac.ac.cn Tel.: +86 43185262964; Fax: +86 431 85689278.

ORCID

Jianshe Huang: 0000-0002-9570-4101

Xiurong Yang: 0000-0003-0021-5135

Notes

The authors declare no competing financial interest.

ACKNOWLEDGMENTS

This work was supported by the National Key Research and Development Program of China (2016YFA0201301), the National Natural Science Foundation of China (nos. 21627808 and 21721003), the Key Research Program of Frontier Sciences, CAS (QYZDY-SSW-SLH019).

REFERENCES

(1) Wu, P.; Hou, X. D.; Xu, J. J.; Chen, H. Y. *Nanoscale* **2016**, *8*, 8427-8442.
(2) Li, L.; Chen, Y.; Zhu, J. J. *Anal. Chem.* **2017**, *89*, 358-371.
(3) Ma, C.; Cao, Y.; Gou, X.; Zhu, J.-J. *Anal. Chem.* **2019**.
(4) Feng, Q. M.; Shen, Y. Z.; Li, M. X.; Zhang, Z. L.; Zhao, W.; Xu, J. J.; Chen, H. Y. *Anal. Chem.* **2016**, *88*, 937-944.
(5) Liang, R. P.; Yu, L. D.; Tong, Y. J.; Wen, S. H.; Cao, S. P.; Qiu, J. D. *Chem. Commun.* **2018**, *54*, 14001-14004.
(6) Ye, J.; Zhu, L.; Yan, M.; Zhu, Q.; Lu, Q.; Huang, J.; Cui, H.; Yang, X. *Anal. Chem.* **2019**, *91*, 1524-1531.
(7) Zhu, L.; Ye, J.; Yan, M.; Zhu, Q.; Yang, X. *Analyst* **2019**, *144*, 6554-6560.
(8) Zhang, H. R.; Xu, J. J.; Chen, H. Y. *Anal. Chem.* **2013**, *85*, 5321-5325.
(9) Cheng, Y.; Huang, Y.; Lei, J.; Zhang, L.; Ju, H. *Anal. Chem.* **2014**, *86*, 5158-5163.
(10) Hao, N.; Li, X. L.; Zhang, H. R.; Xu, J. J.; Chen, H. Y. *Chem. Commun.* **2014**, *50*, 14828-14830.

(11) Zhao, H. F.; Liang, R. P.; Wang, J. W.; Qiu, J. D. *Chem. Commun.* **2015**, *51*, 12669-12672.
(12) Shao, K.; Wang, B.; Ye, S.; Zuo, Y.; Wu, L.; Li, Q.; Lu, Z.; Tan, X.; Han, H. *Anal. Chem.* **2016**, *88*, 8179-8187.
(13) Wang, Y. Z.; Hao, N.; Feng, Q. M.; Shi, H. W.; Xu, J. J.; Chen, H. Y. *Biosens. Bioelectron.* **2016**, *77*, 76-82.
(14) Feng, X.; Gan, N.; Zhang, H.; Li, T.; Cao, Y.; Hu, F.; Jiang, Q. *Biosens. Bioelectron.* **2016**, *75*, 308-314.
(15) Lin, Y.; Wang, J.; Luo, F.; Guo, L.; Qiu, B.; Lin, Z. *Electrochim. Acta* **2018**, *283*, 798-805.
(16) Lin, Y.; Jia, J. P.; Yang, R.; Chen, D. Z.; Wang, J.; Luo, F.; Guo, L. H.; Qiu, B.; Lin, Z. Y. *Anal. Chem.* **2019**, *91*, 3717-3724.
(17) Zhu, L.; Ye, J.; Wang, S.; Yan, M.; Zhu, Q.; Huang, J.; Yang, X. *Chem. Commun.* **2019**, *55*, 11551-11554.
(18) Guo, W.; Ding, H.; Gu, C.; Liu, Y.; Jiang, X.; Su, B.; Shao, Y. *J. Am. Chem. Soc.* **2018**, *140*, 15904-15915.
(19) Yin, P.; Choi, H. M. T.; Calvert, C. R.; Pierce, N. A. *Nature* **2008**, *451*, 318-U314.
(20) Li, B.; Ellington, A. D.; Chen, X. *Nucleic Acids Res.* **2011**, *39*, e110.
(21) Liu, J.; Zhang, Y.; Xie, H.; Zhao, L.; Zheng, L.; Ye, H. *Small* **2019**, e1902989.
(22) Chen, X.; Briggs, N.; McLain, J. R.; Ellington, A. D. *Proc. Natl. Acad. Sci. U. S. A.* **2013**, *110*, 5386-5391.
(23) Bartel, D. P. *Cell* **2004**, *116*, 281-297.
(24) Dong, H.; Lei, J.; Ding, L.; Wen, Y.; Ju, H.; Zhang, X. *Chem. Rev.* **2013**, *113*, 6207-6233.
(25) Lu, C. H.; Li, J.; Lin, M. H.; Wang, Y. W.; Yang, H. H.; Chen, X.; Chen, G. N. *Angew. Chem. Int. Ed. Engl.* **2010**, *49*, 8454-8457.
(26) Yu, S.; Wang, Y.; Jiang, L. P.; Bi, S.; Zhu, J. J. *Anal. Chem.* **2018**, *90*, 4544-4551.
(27) Hao, N.; Dai, P. P.; Yu, T.; Xu, J. J.; Chen, H. Y. *Chem. Commun.* **2015**, *51*, 13504-13507.
(28) Liu, H.; Tian, T.; Zhang, Y.; Ding, L.; Yu, J.; Yan, M. *Biosens. Bioelectron.* **2017**, *89*, 710-714.
(29) Zhang, H. M.; Wang, K. Y.; Bu, S. J.; Li, Z. Y.; Ju, C. J.; Wan, J. Y. *Mol. Cell. Probes* **2018**, *38*, 13-18.
(30) Guo, Y.; Wu, J.; Ju, H. *Chem. Sci.* **2015**, *6*, 4318-4323.
(31) Wang, J.; Pan, M.; Wei, J.; Liu, X.; Wang, F. *Chem. Commun.* **2017**, *53*, 12878-12881.
(32) Tang, Y.; Lu, B.; Zhu, Z.; Li, B. *Chem. Sci.* **2018**, *9*, 760-769.
(33) Wang, H.; Li, C.; Liu, X.; Zhou, X.; Wang, F. *Chem. Sci.* **2018**, *9*, 5842-5849.
(34) Tao, C.; Yan, Y.; Xiang, H.; Zhu, D.; Cheng, W.; Ju, H.; Ding, S. *Chem. Commun.* **2015**, *51*, 4220-4222.
(35) Chen, J.; Qiu, H. D.; Zhang, M. L.; Gu, T. N.; Shao, S. J.; Huang, Y.; Zhao, S. L. *Biosens. Bioelectron.* **2015**, *68*, 550-555.

(36) Quan, K.; Huang, J.; Yang, X.; Yang, Y.; Ying, L.; Wang, H.; He, Y.; Wang, K. *Chem. Commun.* **2015**, *51*, 937-940.
(37) D'Alessandra, Y.; Devanna, P.; Limana, F.; Straino, S.; Di Carlo, A.; Brambilla, P. G.; Rubino, M.; Carena, M. C.; Spazzafumo, L.; De Simone, M.; Micheli, B.; Biglioli, P.; Achilli, F.; Martelli, F.; Maggiolini, S.; Marenzi, G.; Pompilio, G.; Capogrossi, M. C. *Eur. Heart J.* **2010**, *31*, 2765-2773.
(38) Wang, G. K.; Zhu, J. Q.; Zhang, J. T.; Li, Q.; Li, Y.; He, J.; Qin, Y. W.; Jing, Q. *Eur. Heart J.* **2010**, *31*, 659-666.
(39) Cheng, M.; Yang, J.; Zhao, X.; Zhang, E.; Zeng, Q.; Yu, Y.; Yang, L.; Wu, B.; Yi, G.; Mao, X.; Huang, K.; Dong, N.; Xie, M.; Limdi, N. A.; Prabhu, S. D.; Zhang, J.; Qin, G. *Nat Commun* **2019**, *10*, 959.
(40) Jie, G.; Ge, J.; Gao, X.; Li, C. *Biosens. Bioelectron.* **2018**, *118*, 115-121.
(41) Cao, W. D.; Ferrance, J. P.; Demas, J.; Landers, J. P. *J. Am. Chem. Soc.* **2006**, *128*, 7572-7578.
(42) Simmel, F. C.; Yurke, B.; Singh, H. R. *Chem. Rev.* **2019**, *119*, 6326-6369.
(43) Jiang, Y. S.; Bhadra, S.; Li, B.; Ellington, A. D. *Angew. Chem. Int. Ed. Engl.* **2014**, *53*, 1845-1848.

For TOC only